

Comments and Corrections to “Capacity of Multiple-Antenna Systems With Both Receiver and Transmitter Channel State Information”

Kamal Singh, Chandradeep Singh

Abstract

In this correspondence, we correct the ergodic capacity versus SNR curves of the coherent multiple-input multiple-output (MIMO) channel in independent and identically distributed (IID) Rayleigh fading in the correspondence cited in the title [1]. More importantly, the corrected capacity results present an interesting and compelling contrast between performances of the coherent MIMO systems with and without channel state information at the transmitter; whereas this view is somewhat limited in [1] because of flaws in the capacity curves.

Index Terms

Ergodic capacity, multiple-input multiple-output (MIMO), Rayleigh fading channel, power control, channel state information at the transmitter (CSIT).

I. INTRODUCTION

THE main objective of this note is to correct the ergodic capacity versus SNR graphs of the MIMO fading channel in [1]. The ergodic capacity of a coherent MIMO fading channel \mathbf{H} ¹ with perfect instantaneous channel state information \mathbf{H} at the transmitter (CSIT) can be obtained by solving the following problem² [3, Section 8.2]:

$$\max_{Q(\mathbf{H}) : \text{Tr}(\mathbb{E}_{\mathbf{H}}[Q(\mathbf{H})]) \leq P} \mathbb{E}_{\mathbf{H}}[\log \det(\mathbf{I}_{N_R} + \mathbf{H}Q(\mathbf{H})\mathbf{H}^\dagger)] \quad (1)$$

where $Q(\mathbf{H})$ is the input covariance matrix and P is an average power constraint at the transmitter, which implies $\text{Tr}(\mathbb{E}_{\mathbf{H}}[Q(\mathbf{H})]) \leq P$. In [1], the authors solved the optimization in (1) for the IID Rayleigh fading model, i.e. channel matrix \mathbf{H} has i.i.d. entries and each entry in $\mathbf{H} \sim \mathcal{CN}(0, 1)$, to yield the capacity with CSIT as

$$C = m \mathbb{E}_{\lambda}[\log(1 + \lambda P(\lambda))] \quad (2)$$

where $m = \min(N_R, N_T)$ and the optimal *waterfilling* power scheme $P(\lambda) = (1/\lambda_0 - 1/\lambda)^+$. We will use explicit notation $C(x, y, z)$ (resp. $\tilde{C}(x, y, z)$) to denote the capacity of this $x \times y$ MIMO fading channel with CSIT (resp. without CSIT) under constraint z on the average transmit power. Precisely, the ergodic capacity has an integral-form expression as given in the Eq. (58) in [1], and is reproduced here with a simple change of variables³ as follows:

$$C(N_R, N_T, P) = m \int_{\lambda_0}^{\infty} \log\left(\frac{\lambda}{\lambda_0}\right) f_{\lambda}(\lambda) d\lambda \quad (3)$$

where λ_0 is the cutoff parameter determined from

$$\int_{\lambda_0}^{\infty} \left(\frac{1}{\lambda_0} - \frac{1}{\lambda}\right) f_{\lambda}(\lambda) d\lambda = \frac{P}{m} \quad (4)$$

¹The matrix \mathbf{H} is a $N_R \times N_T$ matrix, where N_R and N_T indicate the number of receive and transmit antennas, respectively.

²Covariance matrix of the receiver AWGN noise vector, generally denoted as $N_0 \mathbf{I}_{N_R}$ in the literature, is taken to be the identity i.e. $N_0 = 1$.

³The γ variable in the Eq. (58) in [1] and λ variable in (3) above are related as $\gamma = \lambda P / (m N_0)$.

and the eigenmode distribution $f_\lambda(\lambda)$ is given by

$$f_\lambda(\lambda) = \frac{e^{-\lambda} \lambda^{n-m}}{m} \sum_{k=0}^{m-1} \frac{k!}{(k+n-m)!} [L_k^{n-m}(\lambda)]^2 \quad (5)$$

where, in turn, $n = \max(N_R, N_T)$ and $L_k^{n-m}(\lambda)$, the associated Laguerre polynomial of order k , has a closed-form expression given as

$$L_k^{n-m}(\lambda) = \sum_{p=0}^k \frac{(-\lambda)^p}{p!} \binom{k+n-m}{k-p}. \quad (6)$$

The ergodic capacity of this coherent MIMO channel *without* CSIT is given by

$$\widehat{C}(N_R, N_T, P) = m \int_0^\infty \log(1 + P\lambda/N_T) f_\lambda(\lambda) d\lambda \quad (7)$$

and the optimal power allocation is obtained by dividing the total transmit power P equally among all transmit antennas [2, Theorem 2].

It is easy to verify that

$$C(N_R, N_T, P) = C(N_T, N_R, P), \quad (8)$$

and

$$\widehat{C}(N_R, N_T, P) \neq \widehat{C}(N_T, N_R, P) \quad (9)$$

holds in general, except with equality when $N_R = N_T$. In fact, it is easy to check that for $N_R > N_T$,

$$\widehat{C}(N_R, N_T, P) > \widehat{C}(N_T, N_R, P) \text{ holds.} \quad (10)$$

In the following, for simplicity of notation, we will drop the functional dependence so that C and \widehat{C} should be understood to refer to $C(N_R, N_T, P)$ and $\widehat{C}(N_R, N_T, P)$ respectively. In the next section, we present counter ergodic capacity results with detailed justifications followed by comparison with the existing curves in the correspondence cited in the title. The note concludes with a brief discussion and implication of the corrected capacity results with and without CSIT.

II. COUNTER RESULTS

The focus is on the ergodic capacity versus SNR curves for the MIMO Rayleigh channel with CSIT presented in the Fig. 5 (or Fig. 6) in [1]. In this section, we present counter results for the ergodic capacity of the MIMO Rayleigh channel with CSIT computed using two independent approaches: *one* set of results is computed using standard root-finding algorithms to evaluate the waterfilling level $1/\lambda_0$ in (4) and then using numerical integration in (3), and the *second* set of results using Monte Carlo simulation⁴. The range of SNR⁵, N_T and N_R are chosen as identical to that in [1]. The computed values with these two methods are close and thus, suggesting the correctness of the results; precisely, the values match exactly up to 2 decimal places, see Table I-Table V.

⁴10⁶ samples are considered for Monte Carlo simulations.

⁵SNR is taken as $P/(mN_0)$, similar to as Eq. (34) in [1].

TABLE I: $N_R = 4, N_T = 4$

SNR (dB)	Capacity (Monte Carlo) (bits/s/Hz)	Capacity (Numerical) (bits/s/Hz)
-15	1.182976	1.182924
-10	2.518979	2.519749
-5	4.788550	4.789042
0	8.141317	8.141885
5	12.502087	12.506322
10	17.699588	17.695610

TABLE II: $N_R = 4, N_T = 6$

SNR (dB)	Capacity (Monte Carlo) (bits/s/Hz)	Capacity (Numerical) (bits/s/Hz)
-15	1.461202	1.461242
-10	3.108600	3.108137
-5	5.894179	5.894378
0	9.973844	9.974640
5	15.256107	15.255904
10	21.346760	21.346403

TABLE III: $N_R = 4, N_T = 8$

SNR (dB)	Capacity (Monte Carlo) (bits/s/Hz)	Capacity (Numerical) (bits/s/Hz)
-15	1.714074	1.714015
-10	3.633365	3.634128
-5	6.858986	6.859198
0	11.528260	11.527121
5	17.324821	17.326976
10	23.673975	23.674296

TABLE IV: $N_R = 4, N_T = 10$

SNR (dB)	Capacity (Monte Carlo) (bits/s/Hz)	Capacity (Numerical) (bits/s/Hz)
-15	1.949946	1.949609
-10	4.120259	4.120068
-5	7.730976	7.732018
0	12.835914	12.836162
5	18.886564	18.886957
10	25.328800	25.329797

TABLE V: $N_R = 4, N_T = 12$

SNR (dB)	Capacity (Monte Carlo) (bits/s/Hz)	Capacity (Numerical) (bits/s/Hz)
-15	2.171655	2.172626
-10	4.576217	4.574792
-5	8.530615	8.530668
0	13.934214	13.933461
5	20.122317	20.121336
10	26.612371	26.613163

The numerically solved capacity with CSIT in Table I-Table V are plotted in Fig. 1 and Fig. 2 along with the corresponding capacity *without* CSIT. The capacity results without CSIT are determined by solving

the integral in (7) numerically and are also verified with Monte Carlo simulations, see Table VI-Table XIV in Appendix A.

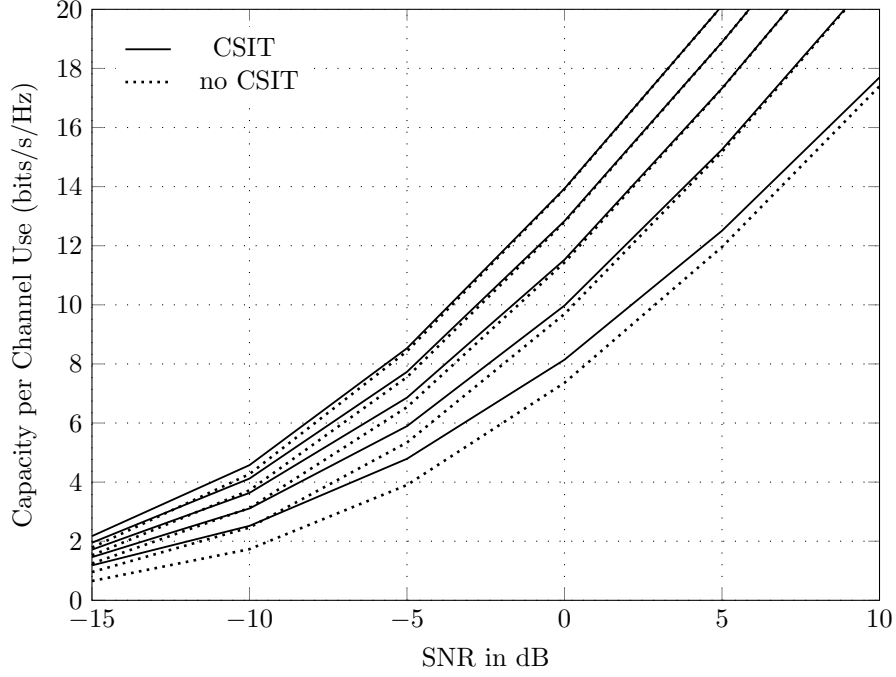


Fig. 1: Ergodic capacity of *coherent* $N_R \times N_T$ MIMO IID Rayleigh channel with $N_T = 4$ (fixed). For each case (CSIT or no CSIT), the curves correspond, in ascending order, to $N_R = 4, 6, 8, 10, 12$.

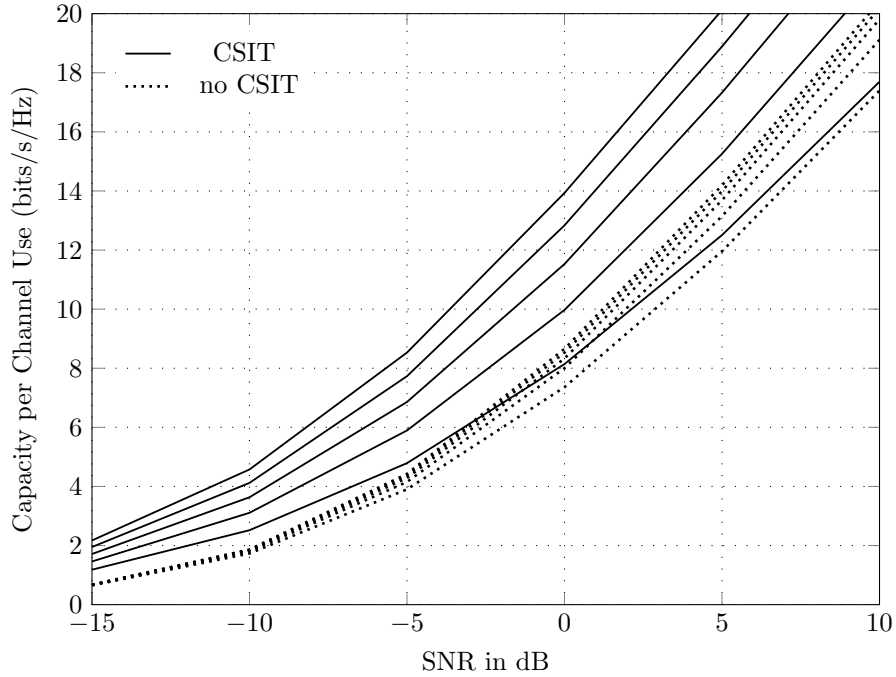


Fig. 2: Ergodic capacity of *coherent* $N_R \times N_T$ MIMO IID Rayleigh channel with $N_R = 4$ (fixed). For each case (CSIT or no CSIT), the curves correspond, in ascending order, to $N_T = 4, 6, 8, 10, 12$.

To further validate the capacity results with CSIT as shown in Fig. 1 (or Fig. 2), we focus on the extreme SNR regimes.

- In the *high* SNR regime, the optimal waterfilling scheme allocates nearly same power for *all* states i.e. $P(\lambda) \approx P/m$ [3, pp. 346-348]. Thus, at high SNR,

$$\begin{aligned} C &= m \mathbb{E}_{\lambda} [\log(1 + \lambda P(\lambda))] \\ &\approx m \int_0^{\infty} \log(1 + P\lambda/m) f_{\lambda}(\lambda) d\lambda. \end{aligned} \quad (11)$$

Comparing (11) with (7), it is straightforward that, at high SNR,

$$C \approx \hat{C} \quad (12)$$

whenever $m = N_T$. This fact, clearly visible in Fig. 1 at high SNRs, validates the correctness of the capacity values with CSIT presented in this note.

- In the *low* SNR regime, [4] showed that the ergodic capacity with CSIT of this MIMO fading channel scales asymptotically as $\text{SNR} \log(1/\text{SNR})^6$; in particular, an on-off transmission scheme on the strongest eigenmode⁷ (say λ_{max}) is proposed that is “asymptotically (at low SNR) capacity-achieving”. This observation is also hinted in [3, Eq. (7.15)]. The ergodic rate achievable with the on-off transmission scheme is given by [4]

$$\begin{aligned} R &= \mathbb{E}_{\lambda_{max}} [\log(1 + \lambda_{max} P(\lambda_{max}))] \\ &= \int_{\tau}^{\infty} \log(1 + P_0 \lambda) f_{\lambda_{max}}(\lambda) d\lambda \end{aligned} \quad (13)$$

where τ is the cutoff parameter (chosen same as the *waterfilling* cutoff λ_0) and $P_0 = P / \int_{\tau}^{\infty} f_{\lambda_{max}}(\lambda) d\lambda$. These rates are obtained for a wide range of low SNR values and plotted in Fig. 3 along with corresponding ergodic capacity with CSIT achieved using the ‘optimal’ waterfilling scheme over all the non-zero eigenmodes.

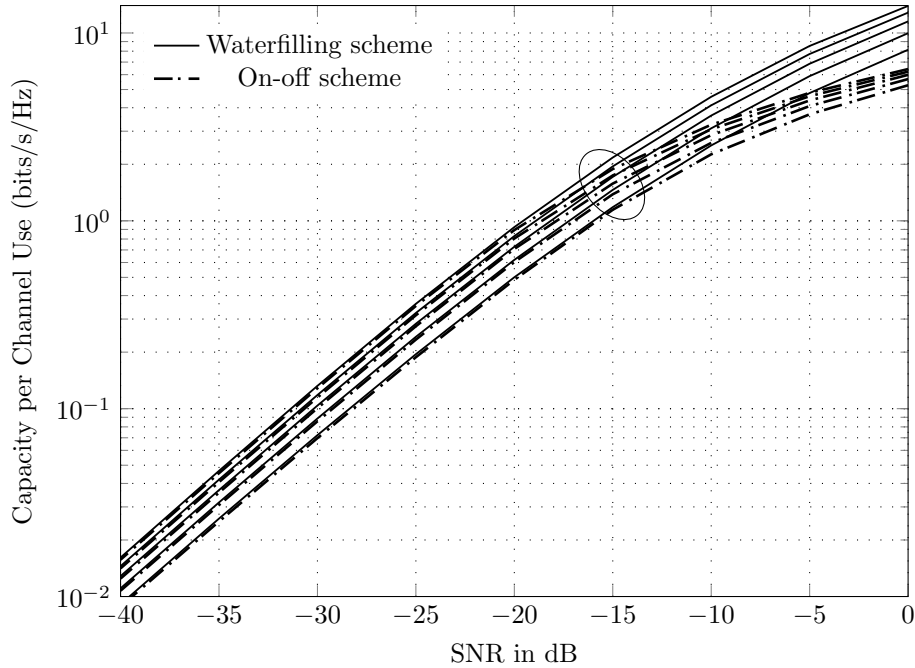


Fig. 3: Ergodic capacity of *coherent* $N_R \times N_T$ MIMO IID Rayleigh channel with CSIT and $N_R = 4$ (fixed) at *low* SNRs. For each case (On-off or Waterfilling), the curves correspond, in ascending order, to $N_T = 4, 6, 8, 10, 12$.

⁶ P/N_0 is taken as SNR in [4]

⁷The CDF of λ_{max} is borrowed from [5, Eq. (6)]

The on-off power scheme rates are close to the computed capacity values with CSIT at sufficiently low SNRs; for example, observe the rates in Fig. 3 at the SNR of -15 dB or lower (for exact comparison, see Table XV-Table XIX in Appendix B). This further validates the correctness of the capacity results with CSIT presented here.

A close examination of the ergodic capacity versus SNR curves in the Fig. 5 and Fig. 6 in [1], when compared with Fig. 1 and Fig. 2 respectively in this note, indicates several differences as follows:

- At low SNRs, the capacity values with CSIT in the Fig. 5 in [1] show significantly ‘larger’ improvements with increasing N_R receive antennas than the corresponding values in Fig. 1 in this note. For example, at low enough SNR of -15 dB, the capacity with CSIT in the Fig. 5 in [1] varies roughly from around 1 to 5 bits/s/Hz as N_R receive antennas increase from 4 to 12 respectively while the corresponding capacity values for these settings in Fig. 1 (or Fig. 3) range nearly from 1.18 to 2.17 bits/s/Hz respectively.
- Though less noticeable, at high SNRs, the capacity values with CSIT in the Fig. 5 in [1] are slightly lower in comparison to the corresponding values in Fig. 1 here.
- Furthermore, the capacity curves *without* CSIT in the Fig. 5 and Fig. 6 in [1] are inaccurate; for example, the $C \approx \bar{C}$ approximation at high SNR whenever $m = N_T$ (as noted in (12)), is missing in the Fig. 5 in [1]. Similar discrepancy can be noticed in the Fig. 6 in [1] by comparing capacity values of the 4×4 Rayleigh channel with and without CSIT at high SNRs ((12) holds for this specific channel setting, but is missing in the Fig. 6 in [1] as well).

In conclusion, there are serious inaccuracies in the ergodic capacity versus SNR graphs (both CSIT and no CSIT) presented in the Fig. 5 and Fig. 6 in [1], thus resulting in unwarranted comparison and conclusion. These graphs are corrected and presented as Fig. 1 and Fig. 2 along with detailed justifications in this note.

III. DISCUSSION

An interesting contrast between performances of the coherent MIMO systems with and without CSIT can be inferred from the corrected capacity curves in Fig. 1 and Fig. 2:

- For the case when the number of receive antennas N_R is kept fixed and number of transmit antennas N_T is increasing (above N_R), the capacity curves without CSIT suggest the effect of varying N_T is marginal. To justify this, notice that the transmit power is spread out equally across all directions in the \mathcal{C}^{N_T} vector space due to the lack of CSIT, leading to ‘wasted’ energy which increases with increasing N_T . On the contrary, the diversity gains possible to the receiver improve due to increasing N_T . Overall, the improvement in the capacity without CSIT is marginal; with CSIT, the vector is projected on only the desirable m non-zero eigenmodes or directions.
- In contrast, for the case when N_T is fixed and N_R is increasing (above N_T), the gap between the capacity curves with CSIT and without CSIT is generally small and nearly vanishes at high SNR (see (12)). At high SNRs, and since $m = N_T$ holds here, it is easy to deduce that the optimal power allocations at the transmit antennas in both situations (CSIT and no CSIT) are nearly identical. Furthermore, with focus on the capacity without CSIT here, notice that the spread of transmit power or energy across all directions in \mathcal{C}^{N_T} remains ‘same’ (since N_T is fixed) while the *coherent* receiver is able to exploit higher diversity gains possible due to increasing N_R .

This overall contrast is somewhat limited in [1] because of flaws in the capacity curves.

The implications of these observations for the coherent MIMO system design can be briefly summarized as follows:

- 1) the loss of capacity due to lack of channel state information at the transmitter side for the MIMO Rayleigh fading channel can be made significantly smaller at *medium to high* SNRs by providing a ‘larger’ antenna array at the receiver⁸.

⁸number of receive antennas to be larger than that of transmit antennas

- 2) On the other hand, larger antenna array at the transmitter yields minimal improvement in the capacity for the lack of CSIT. Alternatively, when the antenna array at the transmitter side is larger than at the receiver end, it is imperative to provide channel information at the transmitter to increase the throughput significantly.

REFERENCES

- [1] S. Jayaweera and H. V. Poor, "Capacity of multiple-antenna systems with both receiver and transmitter channel state information," in *IEEE Transactions on Information Theory*, vol. 49, no. 10, pp. 2697–2709, Oct. 2003.
- [2] E. Telatar, "Capacity of multi-antenna Gaussian channels," in *European Transactions on Telecommunications*, vol. 10, no. 6, pp. 585–595, November-December 1999.
- [3] D. Tse and P. Viswanath, *Fundamentals of wireless communication*. Cambridge university press, 2005.
- [4] A. Tall, Z. Rezki and M.-S. Alouini, "MIMO Channel Capacity with Full CSI at Low SNR," in *IEEE Wireless Communications Letters*, vol. 1, no. 5, pp. 488–491, October 2012.
- [5] Ming Kang and M.-S. Alouini, "A comparative study on the performance of MIMO MRC systems with and without cochannel interference," in *IEEE Transactions on Communications*, vol. 52, no. 8, pp. 1417–1425, Aug. 2004.

APPENDIX A ERGODIC CAPACITY (NO CSIT)

TABLE VI: $N_R = 4, N_T = 4$

SNR (dB)	Capacity (Monte Carlo) (bits/s/Hz)	Capacity (Numerical) (bits/s/Hz)
-15	0.653249	0.653210
-10	1.731278	1.731566
-5	3.901254	3.901646
0	7.360472	7.360570
5	11.954841	11.958356
10	17.402147	17.398369

TABLE VII: $N_R = 4, N_T = 6$

SNR (dB)	Capacity (Monte Carlo) (bits/s/Hz)	Capacity (Numerical) (bits/s/Hz)
-15	0.664150	0.664113
-10	1.796232	1.796320
-5	4.152699	4.153194
0	8.004090	8.003924
5	13.143525	13.143428
10	19.114700	19.114446

TABLE VIII: $N_R = 4, N_T = 8$

SNR (dB)	Capacity (Monte Carlo) (bits/s/Hz)	Capacity (Numerical) (bits/s/Hz)
-15	0.669718	0.669736
-10	1.830347	1.830585
-5	4.287120	4.287054
0	8.331369	8.330539
5	13.683868	13.685661
10	19.806269	19.806603

TABLE IX: $N_R = 4, N_T = 10$

SNR (dB)	Capacity (Monte Carlo) (bits/s/Hz)	Capacity (Numerical) (bits/s/Hz)
-15	0.673125	0.673167
-10	1.851860	1.851785
-5	4.369483	4.369846
0	8.525321	8.525929
5	13.991696	13.992216
10	20.179583	20.179123

TABLE X: $N_R = 4, N_T = 12$

SNR (dB)	Capacity (Monte Carlo) (bits/s/Hz)	Capacity (Numerical) (bits/s/Hz)
-15	0.675493	0.675479
-10	1.866260	1.866194
-5	4.426025	4.426032
0	8.655543	8.655479
5	14.188157	14.188736
10	20.413271	20.412153

TABLE XI: $N_R = 6, N_T = 4$

SNR (dB)	Capacity (Monte Carlo) (bits/s/Hz)	Capacity (Numerical) (bits/s/Hz)
-15	0.956394	0.956307
-10	2.462461	2.462844
-5	5.339700	5.340373
0	9.687900	9.688512
5	15.175786	15.175911
10	21.334315	21.332693

TABLE XII: $N_R = 8, N_T = 4$

SNR (dB)	Capacity (Monte Carlo) (bits/s/Hz)	Capacity (Numerical) (bits/s/Hz)
-15	1.245405	1.245477
-10	3.122625	3.123057
-5	6.537848	6.537777
0	11.433137	11.432010
5	17.310972	17.311652
10	23.673682	23.672450

TABLE XIII: $N_R = 10, N_T = 4$

SNR (dB)	Capacity (Monte Carlo) (bits/s/Hz)	Capacity (Numerical) (bits/s/Hz)
-15	1.521897	1.521850
-10	3.722394	3.723170
-5	7.553039	7.552851
0	12.800568	12.799501
5	18.881360	18.882073
10	25.330437	25.329254

TABLE XIV: $N_R = 12, N_T = 4$

SNR (dB)	Capacity (Monte Carlo) (bits/s/Hz)	Capacity (Numerical) (bits/s/Hz)
-15	1.786068	1.786435
-10	4.272003	4.272138
-5	8.429043	8.428782
0	13.916139	13.916232
5	20.120091	20.119217
10	26.612370	26.612935

APPENDIX B

ERGODIC CAPACITY (ON-OFF & WATERFILLING SCHEME)

TABLE XV: $N_R = 4, N_T = 4$

SNR (dB)	Capacity (Waterfilling) (bits/s/Hz)	On-off rate (Monte-carlo) (bits/s/Hz)	On-off rate (numerical) (bits/s/Hz)
0	8.141455	5.270533	5.264009331
-5	4.788881	3.691180	3.684889873
-10	2.519896	2.259619	2.254272476
-15	1.182636	1.145351	1.141753736
-20	0.500745	0.485424	0.483608496
-25	0.195009	0.187945	0.187270682
-30	0.072300	0.069711	0.069370405
-35	0.025994	0.025088	0.024979542
-40	0.009099	0.008847	0.008820817

TABLE XVI: $N_R = 4, N_T = 6$

SNR (dB)	Capacity (Waterfilling) (bits/s/Hz)	On-off rate (Monte-carlo) (bits/s/Hz)	On-off rate (numerical) (bits/s/Hz)
0	9.974868	5.683648	5.677020344
-5	5.894041	4.083595	4.077349245
-10	3.107786	2.599575	2.593966946
-15	1.461355	1.384511	1.380272409
-20	0.619716	0.603249	0.600875364
-25	0.241313	0.233272	0.232197311
-30	0.088662	0.085671	0.085386323
-35	0.031695	0.030700	0.030499115
-40	0.011062	0.010743	0.010684742

TABLE XVII: $N_R = 4, N_T = 8$

SNR (dB)	Capacity (Waterfilling) (bits/s/Hz)	On-off rate (Monte-carlo) (bits/s/Hz)	On-off rate (numerical) (bits/s/Hz)
0	11.527083	5.985882	5.979340923
-5	6.859201	4.374472	4.368011005
-10	3.633938	2.859162	2.853247814
-15	1.714000	1.578669	1.574165663
-20	0.727666	0.708751	0.706173821
-25	0.283272	0.274775	0.273769589
-30	0.103875	0.100618	0.100242818
-35	0.036873	0.035746	0.035616903
-40	0.012848	0.012466	0.012410698

TABLE XVIII: $N_R = 4$, $N_T = 10$

SNR (dB)	Capacity (Waterfilling) (bits/s/Hz)	On-off rate (Monte-carlo) (bits/s/Hz)	On-off rate (numerical) (bits/s/Hz)
0	12.836196	6.226041	6.219488459
-5	7.731536	4.606987	4.600511855
-10	4.119671	3.070413	3.064576730
-15	1.949462	1.743438	1.738625987
-20	0.829473	0.805049	0.802063549
-25	0.323232	0.314441	0.313158002
-30	0.118232	0.114694	0.114363686
-35	0.041907	0.040672	0.040480673
-40	0.014515	0.014124	0.014049351

TABLE XIX: $N_R = 4$, $N_T = 12$

SNR (dB)	Capacity (Waterfilling) (bits/s/Hz)	On-off rate (Monte-carlo) (bits/s/Hz)	On-off rate (numerical) (bits/s/Hz)
0	13.933972	6.426369	6.419435968
-5	8.531219	4.801641	4.795005000
-10	4.574472	3.249739	3.243676350
-15	2.172983	1.887175	1.882104161
-20	0.925992	0.893189	0.890072923
-25	0.361619	0.352384	0.350926130
-30	0.132287	0.128491	0.127962447
-35	0.046683	0.045373	0.045165040
-40	0.016133	0.015711	0.015626368